Supplemental material to this article can be found at:
http://molpharm.aspetjournals.org/content/suppl/2007/05/16/mol.106.032458.DC1

0026-895X/07/7202-407–417$20.00
MOLECULAR PHARMACOLOGY
Copyright © 2007 The American Society for Pharmacology and Experimental Therapeutics
Mol Pharmacol 72:407–417, 2007

Vol. 72, No. 2
32458/3233387
Printed in U.S.A.

Glitazones Induce Astroglioma Cell Death by Releasing Reactive Oxygen Species from Mitochondria: Modulation of Cytotoxicity by Nitric Oxide[S]

José M. Pérez-Ortiz, Pedro Tranque, Miguel Burgos, Cecilia F. Vaquero, and Juan Llopis

Physiology Unit, Facultad de Medicina, and Centro Regional de Investigaciones Biomédicas, Universidad de Castilla-La Mancha, Albacete, Spain

Received November 8, 2006; accepted May 15, 2007

ABSTRACT

The glitazones (or thiazolidinediones) are synthetic compounds used in type-2 diabetes, but they also have broad antiproliferative and anti-inflammatory properties still not well understood. We described previously the apoptotic effects of glitazones on astroglioma cells (*J Biol Chem* **279:**8976–8985, 2004). At certain concentrations, we found a selective lethality on glioma cells versus astrocytes that was dependent on a rapid production of reactive oxygen species (ROS) and seemed unrelated to the receptor peroxisome proliferator activated receptor-γ. The present study was aimed at characterizing the oxygen derivatives induced by ciglitazone, rosiglitazone, and pioglitazone in C6 glioma cells and to investigate their intracellular source. We examined the interaction of ROS with nitric oxide (NO) and its consequences for glioma cell survival. Fluorescence microscopy and flow cytometry showed that glitazones induced superoxide anion, peroxynitrite, and hydrogen peroxide, with ciglitazone being the most active. ROS production was completely prevented by uncoupling of the electron transport chain and by removal of glucose as an energy substrate, whereas it was unaffected by inhibition of NADPH-oxidase and xanthine-oxidase. Moreover, glitazones inhibited state 3 respiration in permeabilized cells, and experiments with mitochondrial inhibitors suggested that complex I was the likely target of glitazones. Therefore, these results point to the mitochondrial electron transport chain as the source of glitazone-induced ROS in C6 cells. Glitazones also depolarized mitochondria and reduced mitochondrial pH. NO synthase inhibitors revealed that superoxide anion combines with NO to yield peroxynitrite and that the latter contributes to the cytotoxicity of glitazones in astroglioma cells. Future antitumoral strategies may take advantage of these findings.

The glitazones, also called thiazolidinediones, constitute a group of synthetic compounds with insulin-sensitizing effects. Two members of this family, rosiglitazone and pioglitazone, are approved for the treatment of hyperglycemia in patients with type 2 diabetes mellitus. In most countries, they are used as monotherapy or in combination with sulfonylureas or metformin, and in the United States, they are approved to use in combination with insulin (Yki-Järvinen, 2004). Although the application of glitazones in the clinic is presently limited to diabetes, their potential therapeutic value expands beyond the regulation of the carbohydrate and lipid metabolisms because a growing number of reports have described that glitazones also affect vascular functions, inflammatory processes, cell proliferation, and apoptosis (Feinstein et al., 2005).

Many metabolic and anti-inflammatory properties of glitazones are linked to the activation of the peroxisome proliferator activated receptor-γ (PPARγ), a transcription factor of the nuclear receptor family that not only stimulates but also represses a number of genes (Delerive et al., 2001). However, alternative PPARγ-independent mechanisms are now emerging to account for a set of glitazone responses (Feinstein et

This work was supported by grants from Consejería de Sanidad, JCCM, Spain (refs. 04007-00 and GC04-005) (to J.L.). J.M.P.O. is a fellow from Consejería de Sanidad, Junta de Comunidades de Castilla-La Mancha, Spain (ref. 2006-BIN-1383).

Article, publication date, and citation information can be found at http://molpharm.aspetjournals.org.

doi:10.1124/mol.106.032458.

[S] The online version of this article (available at http://molpharm.aspetjournals.org) contains supplemental material.

ABBREVIATIONS: PPARγ, peroxisome proliferator activated receptor-γ; FCCP, carbonylcyanide *p*-trifluoromethoxyphenyl-hydrazone; DCF, 2′,7′-dichlorofluorescein; $O_2^{\cdot-}$, superoxide anion; H_2DCF, dichlorodihydrofluorescein; H_2DCF-DA, dichlorodihydrofluorescein diacetate; DMNQ, dimethoxynaphtoquinone; HE, hydroethidine; L-NAME, N^{ω}-nitro-L-arginine methyl ester; NOS, nitric-oxide synthase; iNOS, inducible nitric-oxide synthase; $ONOO^-$, peroxynitrite; PI, propidium iodide; ROS, reactive oxygen species; GSNO, *S*-nitrosoglutathione; TMRE, tetramethylrhodamine ethyl ester perchlorate; $\Delta\Psi m$, mitochondrial membrane potential; HBSS, Hanks' balanced salt solution; DMEM, Dulbecco's modified Eagle's medium; 1400W, *N*-(3-(aminomethyl)benzyl)acetamidine.

Downloaded from molpharm.aspetjournals.org at ASPET Journals on September 24, 2017

al., 2005), including antiproliferative and apoptotic actions on several tumor cells in vitro in animal models and in humans (Grommes et al., 2004).

We demonstrated recently that the glitazones ciglitazone and rosiglitazone reduce the viability of astroglial cells (Pérez-Ortiz et al., 2004). This cytotoxic effect was cell-type-dependent, because both glitazones affected preferentially astroglioma cell survival compared with primary rat astrocytes. The mechanism involved in this antitumoral effect was clearly not mediated by PPARγ but seemed related to a short-term generation of reactive oxygen species (ROS) from an unknown cellular source.

Mitochondria are major producers of ROS in response to agents that alter their functions. It is interesting that our preliminary studies found that glitazones can cause mitochondrial membrane depolarization in both glioma cells and astrocytes, pointing to mitochondria as a target of glitazones. In fact, glitazones have been reported to affect mitochondria in hepatoma cells (Masubuchi et al., 2006), Jurkat and Raji cells (Kanunfre et al., 2004), and human multiple myeloma, among others (Ray et al., 2004). Moreover, glitazones have been shown to generate ROS as a result of the modulation of mitochondrial functions in several cell types (Narayanan et al., 2003). On the other hand, glitazones could stimulate ROS production from extramitochondrial sources (i.e., by xanthine-oxidase and NADPH-oxidase, enzymes known to be expressed in astrocytes).

Although we found that ROS are implicated in the lethal effect of glitazones on glioma cells, a matter that still needed clarification is the type of oxygen derivatives released. Superoxide anion ($O_2^{\cdot-}$) is a short-lived ROS generated as a byproduct of oxidative phosphorylation in mitochondria or as a result of the activity of the cytosolic oxidases mentioned before. It can be metabolized to hydrogen peroxide (H_2O_2) by dismutation or converted into peroxynitrite ($ONOO^-$) by combination with NO. In relation to this, the expression of different isoforms of the NO synthase (NOS) in C6 glioma cells has been reported. Both $O_2^{\cdot-}$ derivatives, H_2O_2 and $ONOO^-$, have deleterious effects on cells and could mediate the cytotoxicity of glitazones. NOS activity might modulate glioma cell death caused by glitazones, because H_2O_2 and $ONOO^-$ are expected to induce different levels of toxicity (Radi et al., 2002).

In consequence, the present report was aimed at understanding the actions of glitazones on C6 glioma cells. In particular, we characterized the type of ROS generated in response to glitazones and their subcellular origin. In addition, we addressed the implications of modulating NO levels for the cell lethality induced by glitazones. Our findings indicate a rather selective action of glitazones on mitochondria versus other ROS sources and contribution of both $O_2^{\cdot-}$ and $ONOO^-$ to glitazone cytotoxicity in C6 glioma cells.

Materials and Methods

Reagents. Ciglitazone {5-[[4-[(1-methylcyclohexyl)methoxy]phenyl]methyl]-1,3-thiazolidine-2,4-dione} and carbonyl cyanide 4-(trifluoromethoxy)phenylhydrazone (FCCP) were purchased from Tocris (Ellisville, MO). Rosiglitazone {5-[[4-[2-(methyl-pyridin-2-yl-amino)ethoxy]phenyl]methyl]thiazolidine-2,4-dione}, pioglitazone {5-[[4-[2-(5-ethylpyridin-2-yl)ethoxy]phenyl]methyl]thiazolidine-2,4-dione}, 1400W, and *S*-nitrosoglutathione (GSNO) were obtained from Alexis (Läufelfingen, Switzerland). All of the fluorescent probes used [dichlorodihydrofluorescein diacetate (H_2DCF-DA), hydroethidine (HE), tetramethylrhodamine ethyl ester (TMRE)] were purchased from Invitrogen (Carlsbad, CA), except 4,5-diaminofluorescein diacetate, which was a generous gift from Dr. Kazuya Kikuchi (Osaka University, Osaka, Japan). Apocynin was acquired from Calbiochem (San Diego, CA). Trypsin-EDTA, DMEM-Ham's F12, fetal bovine serum, and antibiotics were obtained from Lonza Walkersville (Walkersville, MD). Mouse anti-nitrotyrosine antibody was purchased from Hycult Biotechnology (Uden, the Netherlands) and sheep antimouse IgG-horseradish peroxidase was from GE Healthcare (Chalfont St. Giles, Buckinghamshire, UK). All other chemicals and inhibitors were purchased from Sigma (St. Louis, MO).

Rat C6 Glioma Cells. The rat astroglioma cell line C6 was cultured in Dulbecco's modified Eagle's medium-Ham's F12 supplemented with 10% fetal bovine serum and antibiotics. Experimental treatments were applied to 60 to 70% confluent cultures.

Measurement of Mitochondrial Membrane Potential. C6 cells were grown in 22-mm round coverslips, and 24 to 36 h after seeding, cells were washed twice with Hanks' balanced salt solution (HBSS) containing 5 mM glucose and 10 mM HEPES, pH 7.4. Cells were loaded with 0.1 μM TMRE for 20 min at room temperature and protected from direct light. After that, coverslips were transferred to a microscopy chamber (Attofluor; Invitrogen) and maintained in the presence of 0.1 μM TMRE. Cell fluorescence was imaged with an epifluorescence inverted microscope (DMIRE-2; Leica, Wetzlar, Germany) equipped with an oil immersion 40× objective (numerical aperture, 1.25). Excitation light at 545 nm was obtained using a monochromator (Hamamatsu Photonics, Shizuoka, Japan) and emitted light was collected by a charge-coupled device camera (Orca-ER; Hamamatsu Photonics). The interference filter used for emission was 635 ± 27 nm, and the dichroic mirror was 570DRL (Omega Optical, Brattleboro, VT). Regions of interest (nucleus and cytoplasm) were selected manually, and pixel intensities were spatially averaged after background subtraction. A binning of two was used to improve the signal-to-noise ratio and minimize photobleaching of TMRE and photodamage to the cells. All images and data were acquired and analyzed using the Aquacosmos software (Hamamatsu Photonics).

Detection of Intracellular ROS by Microscopy and Flow Cytometry. Cells were incubated with the cell-permeant dye H_2DCF-DA, which intracellularly de-esterifies to dichlorodihydrofluorescein (H_2DCF). Reactive oxygen species oxidize H_2DCF to the brightly green fluorescent compound 2′,7′-dichlorofluorescein (DCF), which was monitored by microscopy and flow cytometry following methods described previously (Pérez-Ortiz et al., 2004). For microscopy, C6 cells were grown in 22-mm round coverslips, and 24 to 36 h after seeding, cells were incubated for 30 min with a 20 μM concentration of the corresponding glitazone at 37°C in serum-free DMEM-Ham's F12. Within the last 15 min of glitazone treatment, cells were loaded with 1 μM H_2DCF-DA. Afterward, coverslips were transferred to a microscopy chamber and maintained in HBSS containing 2 mM calcium and 10 mM HEPES, pH 7.4. Cell fluorescence was imaged with the same setup and software described above, using 480 nm excitation (monochromator), 505DRL dichroic mirror, and 535 ± 26 nm emission filter. A binning of four was used to minimize photobleaching of DCF.

For flow cytometry, cells treated with glitazones or vehicle (Me_2SO) were incubated with 2.5 μM H_2DCF-DA for 15 min at 37°C, detached from the plate with trypsin/EDTA, washed with phosphate-buffered saline, resuspended in 1 ml of DMEM-Ham's F12 with 2% fetal bovine serum, and placed on ice protected from light. The intensity of the fluorescent DCF in the cell suspension was measured immediately by a BD-LSR flow cytometer (BD Biosciences, San Jose, CA) equipped with an argon ion laser (488 nm excitation); the emission filter was set at 530 nm. Triplicate samples were run in each experiment, and at least 10,000 cells per sample were analyzed. Mean fluorescence was calculated with the program CellQuest (BD

Downloaded from molpharm.aspetjournals.org at ASPET Journals on September 24, 2017

Biosciences). Dead cells and debris were excluded from the analysis by electronic gating of forward- and side-scattering measurements.

Hydroethidine Staining Assay for Superoxide Formation. Superoxide anion was measured with the fluorescent dye HE. This probe is oxidized to ethidium, which is trapped by intercalating with DNA resulting in a fluorescence signal that can be quantified by flow cytometry. C6 cells were grown in complete DMEM-Ham's F12 and washed with phosphate-buffered saline before treatment. Thereafter, cells were incubated for 15 min with 5 μM HE in serum-free DMEM-Ham's F12 and then treated with each glitazone for 15 min. Afterward, cells were detached from the culture plate with trypsin/EDTA, resuspended in 1 ml of DMEM-Ham's F12 with 2% fetal bovine serum, protected from light, and placed on ice. The intensity of the fluorescent ethidium was measured immediately by a BD-LSR flow cytometer (BD Biosciences) equipped with an argon ion laser (488 nm excitation); the emission filter was set at 575 nm. For imaging HE, cells were loaded with 5 μM HE for 10 min at 37°C in an incubator. After that, coverslips were transferred to a microscopy chamber and maintained in HBSS. Cell fluorescence was imaged with the setup described before. Excitation light was at 397 nm, and emission was collected with a 595 nm emission filter. Regions of interest were selected manually, and pixel intensities were spatially averaged after background subtraction. A binning of two was used to improve the signal-to-noise ratio and minimize photobleaching of HE. All images and data were acquired and analyzed using the Aquacosmos software (Hamamatsu Photonics).

Mitochondrial Respiration. Oxygen consumption of digitonin-permeabilized cells was monitored polarographically with a Clark-type oxygen electrode (Oxygraph, Hansatech Instruments, Norfolk, England) connected to a suitable recorder in a 1-ml thermostated water-jacketed closed chamber with magnetic stirring. The reactions were carried out at 30°C in 1 ml of the standard medium (225 mM sucrose, 10 mM KCl, 5 mM $MgCl_2$, 10 mM KH_2PO_4/K_2HPO_4, 0.1% bovine serum albumin, 1 mM EGTA, and 10 mM Tris-HCl, pH 7.4) containing 10^7 cells; 5 mM pyruvate/2.5 mM malate and 250 μM ADP were added to achieve state 3 of respiration.

NO Analysis with DAF-2. NO production was assayed using the fluorescent probe 4,5-diaminofluorescein (DAF-2). C6 cells were grown in complete DMEM-Ham's F12. After washing with phosphate-buffered saline, cells were incubated with 5 μM 4,5-diaminofluorescein diacetate in DMEM-Ham's F12 serum-free for 15 min followed by the addition of glitazone for another 15 min. Cell fluorescence was analyzed by a BD-LSR flow cytometer (BD Biosciences). Excitation was at 488 nm (argon ion laser), and the emission filter was centered at 530 nm.

Cell Viability by Propidium Iodide Exclusion. This assay is based on the exclusive nuclear labeling of nonviable cells with the DNA intercalating fluorescent dye propidium iodide. C6 glioma cells were harvested with trypsin and stained with 10 μg/ml propidium iodide before analysis by flow cytometry. Fluorescence was excited at 488 nm and measured through a 575 $\pm$ 13 bandpass filter.

Western Blotting. Cell lysates were loaded onto SDS-polyacrylamide gels, electrophoresed, and subsequently transferred to polyvinylidene fluoride membranes (Pall, Ann Arbor, MI), incubated with anti-β-actin (1:2000) or anti-nitrotyrosine (1:50) antibodies, and probed with peroxidase-conjugated secondary antibody following manufacturer's instructions. An enhanced chemiluminescence system was used for visualization.

Statistical Analysis. Results are expressed as a percentage of controls treated with the appropriate vehicle (Me_2SO). Values represent mean $\pm$ S.D. of three to six replicate wells. Data were analyzed by one-way analysis of variance followed by a least significant differences test. Statistical significance of differences versus respective controls is shown (#, $p < 0.05$; *, $p < 0.01$; **, $p < 0.001$; ***, $p < 0.0001$).

Results

Characterization of ROS Induced by Glitazones in C6 Glioma Cells. Our previous work has shown that glitazones generate ROS that cause glioma cell death (Pérez-Ortiz et al., 2004). To further investigate the mechanisms by which glitazones alter glioma cell viability, we first characterized the oxidative-stress response triggered by ciglitazone, rosiglitazone, and pioglitazone. Rat C6 glioma cells were loaded with the ROS-sensitive fluorescent probe H_2DCF in the absence or presence of the different glitazones. The intracellular DCF fluorescence resulting from interaction of H_2DCF with ROS was evaluated by microscopy and flow cytometry. As shown in Fig. 1A, the microscopy images showed an increase in intracellular ROS 1 h after the addition of each glitazone at 20 μM. Quantitative analysis of fluorescence accumulated by cells in these experiments (Fig. 1B) revealed that the maximal increase was achieved by ciglitazone treatment (5.4-fold), followed by rosiglitazone (3.1-fold) and pioglitazone (1.9-fold). Flow cytometry experiments confirmed statistically significant increases in DCF fluorescence 15 min after the addition of any of the glitazones at 20 μM (Fig. 1C). The more robust effect was observed in the ciglitazone-treated group. All glitazones affected ROS production in a dose-dependent manner. At the lowest concentration used (10 μM), ciglitazone induced a highly significant increase in DCF fluorescence ($p < 0.0001$ versus untreated controls), pioglitazone caused a moderate change ($p < 0.05$ versus untreated controls), and rosiglitazone was ineffective.

This analysis was complemented with the measurement of $O_2^{\cdot-}$ by flow cytometry (Fig. 2A). For this purpose, cells were loaded with HE, treated with glitazones, and processed as described for DCF detection. HE fluorescence (488 nm excitation, 575 nm emission) increased markedly with 10 or 20 μM ciglitazone but did not change with either rosiglitazone or pioglitazone. The specificity of HE for $O_2^{\cdot-}$ in live cells is limited by autooxidation and other processes that can yield ethidium. However, $O_2^{\cdot-}$ has been shown to react with HE to form 2-hydroxyethidium, which can be selectively excited at 396 nm with little interference from other oxidation products (Robinson et al., 2006). We used these conditions in imaging experiments because of the lack of an appropriate laser line in our flow cytometer. As a positive control for $O_2^{\cdot-}$ formation, cells were incubated with the redox-cycling dimethoxynaphtoquinone (DMNQ). Figure 2B shows a time course of 2-hydroxyethidium formation, which occurred within minutes of ciglitazone addition. The HE oxidation was more sustained with DMNQ. These results complement the cytometric analysis and support that $O_2^{\cdot-}$ is in fact produced by ciglitazone in C6 cells. In conclusion, this first set of experiments reveals that all glitazones affect ROS production in C6 glioma cells. However, substantial differences among glitazones could be observed, ciglitazone causing higher oxidative stress than rosiglitazone or pioglitazone.

Production of ROS by Glitazones: Need for Functional Mitochondria. It is well-accepted that the mitochondrial electron transport chain is a major endogenous source of ROS (Boveris et al., 1972). Generation of ROS by mitochondria depends on the mitochondrial membrane potential and its electron transport chain flux. Thus, mitochondrial ROS production was shown to decrease exponentially with decreasing mitochondrial transmembrane electric potential

Downloaded from molpharm.aspetjournals.org at ASPET Journals on September 24, 2017

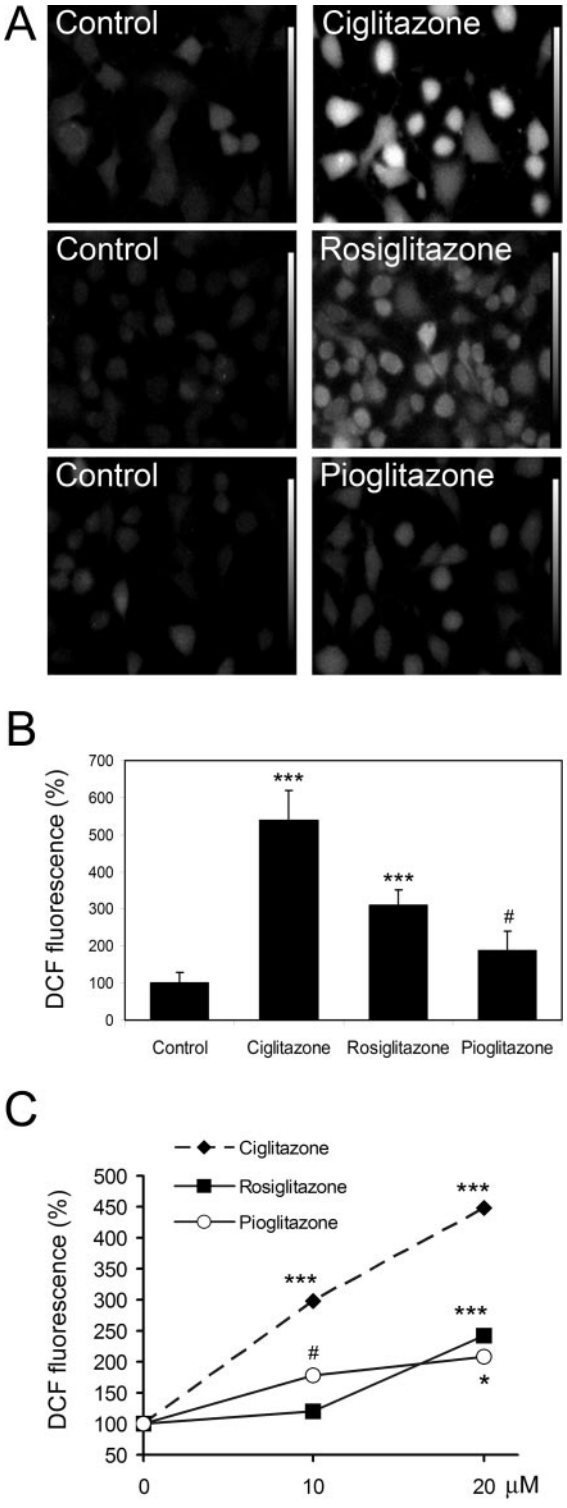

Fig. 1. ROS detection by DCF fluorescence. A, fluorescence microscopy of C6 glioma cells loaded with H_2DCF-DA. Images show the initial DCF fluorescence (control, left), and after a 1-h treatment with 20 μM ciglitazone, rosiglitazone, or pioglitazone (right). Higher fluorescence intensities correspond with higher levels of ROS production. B, quantitation of DCF fluorescence in microscopic images. Intracellular fluorescence values were averaged after background subtraction. C, C6 glioma cells were incubated for 15 min with 10 or 20 μM ciglitazone, rosiglitazone, or pioglitazone in the presence of 2.5 μM H_2DCF-DA, and fluorescence intensity was evaluated by flow cytometry. Results represent mean ± S.D. and are expressed as percentage of controls. Statistical significance of glitazone-treated groups versus untreated controls is indicated (#, $p < 0.05$; ∗, $p < 0.01$; ∗∗∗, $p < 0.0001$).

($\Delta\Psi$m) (Brand et al., 2004). Therefore, to evaluate the implication of mitochondria on glitazone-induced ROS, we examined the effect of altering the mitochondrial membrane potential with FCCP on the ability of ciglitazone to generate ROS. FCCP is a mitochondrial uncoupling agent that acts by carrying protons across the inner mitochondrial membrane. Dissipation of the proton gradient by FCCP leads to a rapid depolarization of mitochondria, acceleration of the electron transport chain, and, consequently, impairment of ROS production by the mitochondria. Therefore, FCCP is expected to inhibit ROS production induced by glitazones if the ROS originate in mitochondria. Figure 3A shows DCF fluorescence of C6 glioma cells after 15-min incubation with 10 μM ciglitazone in the absence or presence of FCCP. Whereas 1 to 2 μM FCCP alone did not alter basal ROS levels, preincubation with FCCP completely inhibited ciglitazone-mediated ROS production. These observations suggest that the mitochondrial electron transport chain is the main source of ROS in C6 glioma cells treated with glitazones. In addition, the availability of energy substrates determines mitochondrial membrane potential and electron transport rate, so that impairment of mitochondria access to fuel severely dampens mitochondrial function and the capacity of mitochondria to produce ROS (Nishikawa et al., 2000). Therefore, to further prove the involvement of mitochondrial electron transport

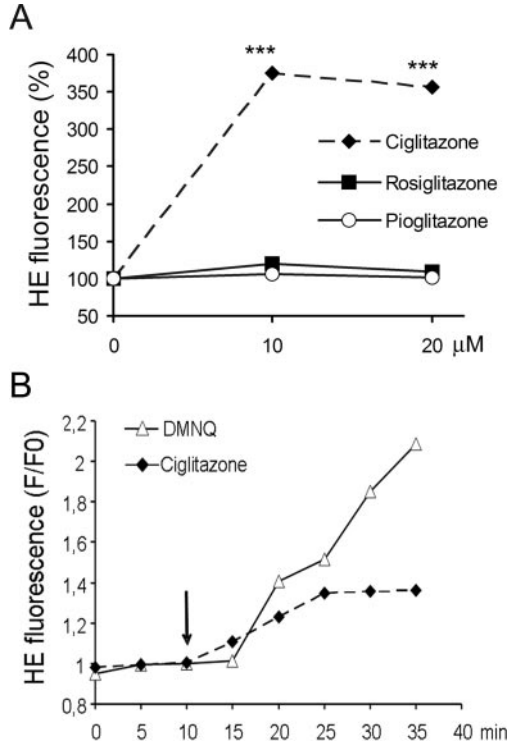

Fig. 2. ROS detection by HE fluorescence. A, C6 glioma cells were incubated for 15 min with 10 or 20 μM ciglitazone, rosiglitazone, or pioglitazone in the presence of 5 μM HE, and fluorescence intensity was evaluated by flow cytometry. Mean values are expressed as a percentage of fluorescence of untreated controls. Statistical significance of glitazone-treated groups versus respective controls is indicated (∗∗∗, $p < 0.0001$). B, time course of HE fluorescence in imaging experiments using excitation at 397 nm and emission at 595 nm on a widefield microscope. C6 cells were treated with 20 μM ciglitazone or DMNQ at time 10 min (arrow). Regions were manually drawn over cells, and fluorescence change over time is expressed as F/F_0 (fluorescence at each time point/initial fluorescence). The mean data of 27 cells from 3 independent experiments (ciglitazone) and 40 cells from 4 experiments (DMNQ) are shown.

Downloaded from molpharm.aspetjournals.org at ASPET Journals on September 24, 2017

chain in the oxidative stress caused by glitazones, we analyzed the consequences of suppressing glucose availability. For these experiments, C6 glioma cells were maintained in HBSS medium with 5.5 mM D-glucose or the nonmetabolizing compound 2-deoxy-glucose. DCF fluorescence recordings after treatment with 10 μM ciglitazone during 15 min are shown in Fig. 3B. 2-Deoxy-glucose completely abrogated the ability of ciglitazone to generate ROS. Removal of D-glucose from the medium produced the same inhibition (data not shown). Moreover, similar results were also obtained using the O_2^- probe HE (data not shown). In conclusion, these experiments further support our previous evidence indicating that the source of glitazone-induced ROS is the mitochondria.

The Electron Transport Chain as the Molecular Target of Glitazones in Mitochondria. Once we determined that ROS synthesis by glitazones is linked to mitochondria, we set up experiments to directly test the influence of glitazones on complex I of the electron transport chain. This respiratory complex is the main mitochondrial site in which ROS can be originated in mammals (Turrens, 2003). Moreover, several agents that interact with complex I are known to increase oxidative stress (Votyakova and Reynolds, 2001; Schönfeld and Reiser, 2006). The effect of glitazones on the oxygen consumption of freshly detached C6 glioma cells was evaluated with an oxygen electrode. Permeabilized cells were energized with complex I substrates (5 mM pyruvate/2.5 mM malate) for 3 min, after which 250 μM ADP was added to induce state 3 of respiration for another 3 min. At that point, the effect of 10 μM ciglitazone, rosiglitazone or pioglitazone treatment on oxygen consumption was evaluated. Results are shown in Fig. 4A as a percentage of untreated controls. Ciglitazone and rosiglitazone decreased the oxygen consumption rate by approximately 27.5 and 21.5%, respectively ($p < 0.01$). In turn, pioglitazone diminished respiration by 18.5% ($p < 0.05$). It is interesting to note that the potency of inhibition was in accordance with the ROS level elicited by each glitazone, suggesting that ROS production can be a consequence of the glitazone inhibition of the electron transport chain.

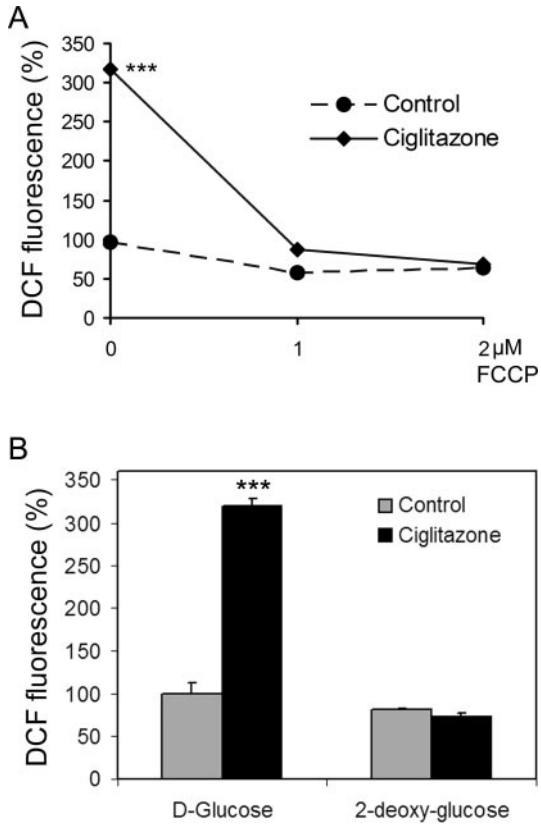

Fig. 3. Influence of mitochondrial electron transport on ROS induction by glitazones. A, DCF fluorescence of C6 glioma cells incubated for 15 min with 10 μM ciglitazone or vehicle (control) was analyzed in the presence of 0, 1, and 2 μM concentrations of the uncoupling agent FCCP by flow cytometry. Results represent means and are expressed as a percentage of untreated cells in the absence of FCCP. This agent completely inhibits the ciglitazone-mediated ROS production, illustrating the dependence of glitazone-induced ROS production on mitochondrial polarity and rate of electron transport. B, DCF fluorescence was examined in C6 glioma cultures after a 15-min treatment with 10 μM ciglitazone or vehicle by flow cytometry. Cells were maintained in HBSS medium with 5.5 mM concentration of either D-glucose or the nonmetabolizing glucose analog 2-deoxy-glucose. Data are presented as a percentage of D-glucose controls and are expressed as mean ± S.D. Asterisks indicate statistical significance of differences with respect to untreated controls (***, $p < 0.0001$). Ciglitazone is unable to generate ROS in the absence of D-glucose, suggesting that mitochondria are the main ROS-generating source.

Inhibition of complex I-dependent oxygen consumption by glitazones prompted us to further analyze the involvement of the mitochondrial electron transport chain complexes in ROS induction. Figure 4B shows the effects of different mitochondrial inhibitors on ciglitazone-evoked ROS production. C6 glioma cell cultures grown to a subconfluent density were incubated with the complex I inhibitor rotenone (2 μM), complex III inhibitor antimycin-A (1 μM) or the ATP synthase inhibitor oligomycin (10 μM). These drugs were also used in combination to assess further inhibition of mitochondrial function. All inhibitors induced significant increases in O_2^- generation when used alone or in combination in a flow cytometry assay using the probe HE. Nevertheless, addition of 10 μM ciglitazone significantly increased O_2^- production beyond the levels achieved by each of the inhibitors alone. In conclusion, none of the inhibitors tested can reproduce the ROS-generating action of glitazones, suggesting that the molecular target of glitazones in mitochondria differs from those of the inhibitors tested. These observations are compatible with an interaction upstream of the rotenone inhibition site in complex I or with a multiplicity of action sites of glitazones in mitochondria.

Glitazones Depolarize Mitochondria and Lower Mitochondrial pH in C6 Glioma Cells. Having shown the implication of the mitochondrial electron transport chain in ROS production induced by glitazones in C6 glioma cells and the likely inhibition at the level of complex I, we next examined whether mitochondrial membrane potential was affected, as would be expected from the proposed mechanism of action. $\Delta\Psi m$ was estimated by fluorescence microscopy using the probe TMRE, a small cationic molecule that accumulates in negatively charged compartments such as the mitochondrial matrix following Nernst's equation. C6 cells were preincubated for 15 min with 0.1 μM TMRE. Subsequent treatment with 10 μM ciglitazone provoked mitochondrial depolarization, detected in the images as a gradual loss of mitochondrial staining, accompanied by an increase in cytoplasmic, nuclear, and extracellular fluorescence resulting from TMRE diffusion (Fig. 5A and Supplemental Fig. S1). Rosiglitazone and pioglitazone also induced mitochondrial depolarization, although the effect was clearly more limited. The mitochondrial uncoupler FCCP (1 μM) was used to pro-

Downloaded from molpharm.aspetjournals.org at ASPET Journals on September 24, 2017

duce a complete loss of ΔΨm after incubation with glitazones. Images showing TMRE fluorescence changes after the addition of glitazones are shown in Fig. 5A, whereas the plots depicted in Fig. 5B illustrate the temporal courses of mitochondrial depolarization. In these recordings, TMRE values were expressed as the nuclear versus perinuclear fluorescence ratio. Nuclear localization of TMRE represents its diffusion from depolarizing mitochondria, whereas perinuclear fluorescence corresponds to polarized mitochondria plus some cytoplasmic diffuse staining. Therefore, increases in the nuclear/perinuclear fluorescence ratio indicate mitochondrial depolarization (as demonstrated in more detail in Supplemental Fig. S1 in a single cell) and thus provide a reliable estimate of the ΔΨm in single cells. Control experiments with FCCP used alone showed that it depolarized mitochondria in seconds and that this effect was reversible upon washing (Supplemental Video). In contrast, the depolarization induced by ciglitazone was not reversed with removal of the drug from the bath in imaging experiments of up to 1-h duration, suggesting that the mechanism of action was different from that of FCCP.

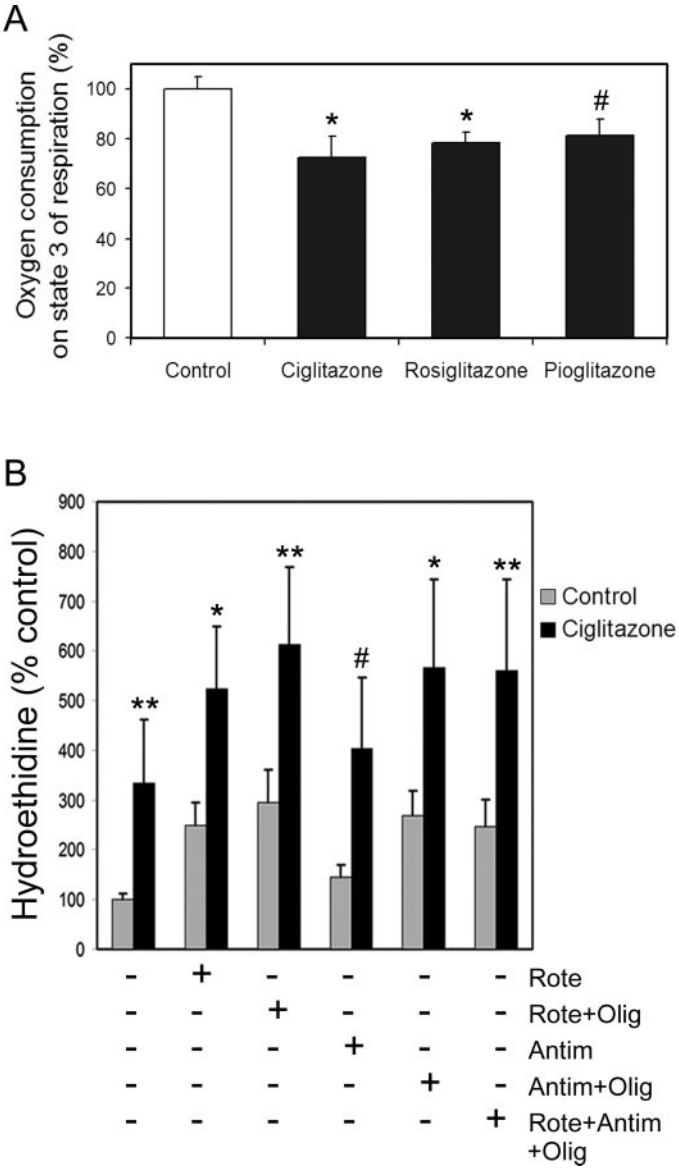

Fig. 4. Effect of glitazones on state 3 of respiration and mitochondrial electron transport chain inhibitors on ciglitazone-induced $O_2^{\cdot-}$ production. A, C6 glioma cells (10^7) freshly detached in 1 ml of standard medium were permeabilized with 40 μM digitonin and immediately used to monitor oxygen consumption. Mitochondria were energized with 5 mM pyruvate/2.5 mM malate (complex I substrates), and ADP (250 μM) was used to induce state 3 of respiration. Ciglitazone, rosiglitazone, pioglitazone (10 μM for all), or vehicle was added to the reaction chamber 3 min after ADP. Results represent mean ± S.D. of oxygen consumption and are expressed as a percentage of untreated controls (#, $p < 0.05$; *, $p < 0.01$). All glitazones inhibit complex I-dependent state 3 of respiration. B, C6 glioma cells were incubated for 15 min with 10 μM ciglitazone or vehicle in the presence of 2 μM rotenone (Rote), 10 μM oligomycin (Olig), and/or 1 μM antimycin-A (Antim) as indicated. $O_2^{\cdot-}$ production was evaluated by flow cytometry after the addition of the fluorescent probe hydroethidine (5 μM) to cell cultures 5 min before initiation of glitazone treatment. Data shown are expressed as a percentage of untreated controls. Statistical significance of ciglitazone-treated groups versus respective controls is shown (#, $p < 0.05$; *, $p < 0.01$; **, $p < 0.001$). None of the mitochondrial inhibitors used, alone or in combination, was able to abolish $O_2^{\cdot-}$ production induced by ciglitazone.

The mitochondrial proton-motive force has two constituents: membrane potential (ΔΨm), and pH gradient across the inner mitochondrial membrane (ΔpHm). We used the recombinant pH indicator "mito-EYFP H148G" (see Supplemental Methods) to determine whether mitochondrial pH was affected by glitazones. Supplemental Fig. S2 shows that ciglitazone (10 μM) decreased resting mitochondrial pH in C6 cells transfected with mito-EYFP H148G. The reduction of mitochondrial pH by ciglitazone occurred concomitantly with the loss of ΔΨm, as was observed in experiments combining imaging of C6 cells transfected with the pH probe and labeled with TMRE (Supplemental Fig. S3), which were well-separated spectrally.

In summary, these results evidence rapid (within minutes) and marked effects of glitazones on ΔΨm and ΔpHm in C6 glioma cells, which were more pronounced with ciglitazone. The reason for this mitochondrial impairment could be the primary block in the electron transport chain described above or secondary damage caused by ROS being released from mitochondria. It is likely that the inhibition of the respiratory chain produces ROS, depolarization, and decrease of mitochondrial ΔpH at the same time.

Extramitochondrial Sources of ROS Are Unresponsive to Ciglitazone. The next set of experiments was designed to test whether extramitochondrial sources of ROS are also responsible for the ROS increase generated by glitazones. Cytosolic NADPH-oxidase and xanthine-oxidase were tested as possible glitazone targets using specific enzyme inhibitors. In these experiments, $O_2^{\cdot-}$ was monitored by flow cytometry with the probe HE. As shown in Supplemental Fig. S4, neither apocynin (20 μM) nor allopurinol (0.1 mM), inhibitors of NADPH-oxidase and xanthine-oxidase, respectively, were able to modify ciglitazone-mediated $O_2^{\cdot-}$ production. These compounds did not have any effect on HE fluorescence by themselves (data not shown). Therefore, glitazones show specificity for mitochondria as their target in relation to ROS production.

NO Modulates $O_2^{\cdot-}$ Production by Glitazones: Implications for Cell Survival. As shown in Fig. 1, DCF fluorescence increased after glitazone treatment, illustrating that at least part of the $O_2^{\cdot-}$ generated by these drugs is converted to H_2O_2 and/or $ONOO^-$. The interaction of $O_2^{\cdot-}$ with NO to form $ONOO^-$ is at least three times faster than $O_2^{\cdot-}$ dismutation, and it has been argued that $ONOO^-$ would be the compound predominantly formed in the presence of NO (Beckman and

Downloaded from molpharm.aspetjournals.org at ASPET Journals on September 24, 2017

Koppenol, 1996). To investigate this issue, we first confirmed the expression of the inducible form of nitric oxide synthase (iNOS) in C6 cells by Western blot. Levels of iNOS in unstimulated C6 cells were significant and exceeded those found in primary astrocyte cultures (Supplemental Fig. S5A). Because one of the downstream effectors of NO is the soluble guanylate cyclase, which yields the second messenger cGMP, we also confirmed the presence of functional iNOS indirectly by quantifying cGMP with an enzyme immunoassay in cell extracts. There was a 9-fold increase in the basal cGMP levels by treatment of C6 cells with tumor necrosis factor-α plus lipopolysaccharide, well-known inducers of iNOS (Supplemental Fig. S5B). Changes in cGMP levels were also measured by fluorescence microscopy in single live cells using the recombinant reporter cygnet-2 (Honda et al., 2001). We found that the NO donor GSNO increased cGMP within minutes of addition to the extracellular medium (data not shown).

To further investigate what O_2^- derivatives are formed in C6 cells upon glitazone exposure and the possible influence of NO in this process, we used flow cytometry with the probe DAF-2 to monitor NO levels after glitazone treatment. DAF-2 reacts with NO in the presence of oxygen, leading to a green fluorescent triazole compound (Nagano, 1999). As a consequence, the reaction of O_2^- with NO to yield $ONOO^-$ is expected to reduce DAF-2 fluorescence. In fact, treatment of C6 glioma cells with 10 μM ciglitazone reduced DAF-2 fluorescence significantly ($p < 0.05$) (Fig. 6A). This decrease in NO is in accordance with the ciglitazone-mediated O_2^- increase detected previously with HE. Therefore, these results suggest that O_2^- released by glitazones is, at least in part, combined with NO to form $ONOO^-$. On the contrary, rosiglitazone and pioglitazone did not affect the DAF-2 signal, in correspondence with the lack of change in O_2^- levels observed with HE fluorescence (Fig. 2A). As a positive control in these assays, C6 glioma cells were also incubated with the NO donor GSNO (500 μM), which markedly increased DAF-2 fluorescence, in agreement with the results obtained with the cGMP sensor, cygnet-2.

As a second approach to study the modulation of glitazone-evoked ROS production by NO, we checked the effect of a decrease in NO on O_2^- levels in C6 glioma cells. NO levels were reduced using the NOS inhibitor N^{ω}-nitro-L-arginine methyl ester (L-NAME) or 1400W, a specific inhibitor of the inducible form, iNOS. The enzyme immunoassay for cGMP described above was used to demonstrate the ability of L-NAME and 1400W to inhibit NO release (stimulated by tu-

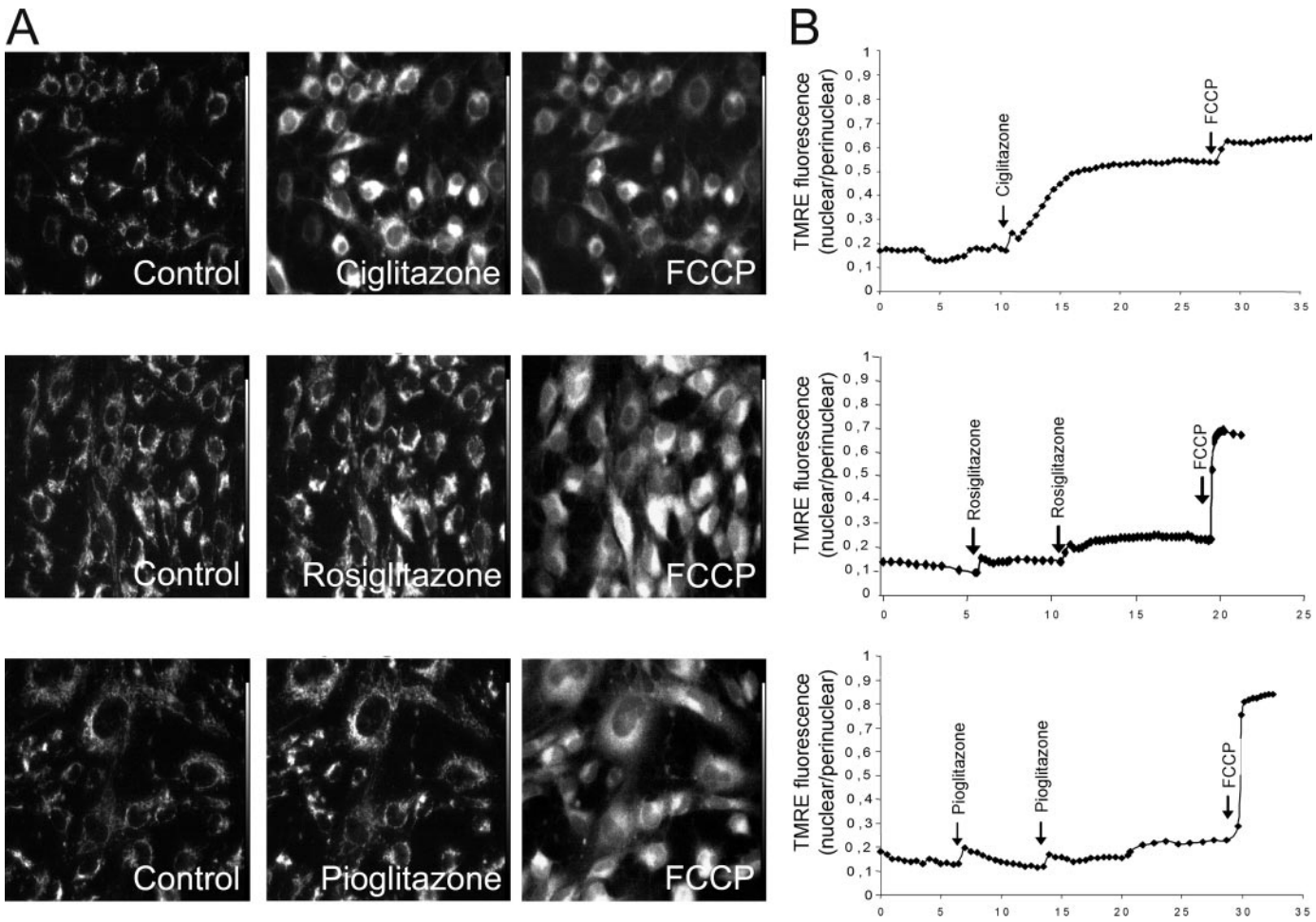

Fig. 5. Temporal courses of mitochondrial depolarization by glitazones. A, fluorescence microscopy images of C6 glioma cells showing the initial TMRE fluorescence state in vehicle-treated controls (left); after 10 μM ciglitazone, rosiglitazone, or pioglitazone treatment (middle); and after the addition of 1 μM FCCP (right). FCCP is herein used as a positive control of mitochondrial depolarization, yielding the maximal fluorescence shift. This is observed as diffusion of staining from the mitochondria to the nucleus and cytosol. B, time course of mitochondrial depolarization after glitazone and FCCP treatments. Results are expressed as mean ± S.D. of the ratio between nuclear and perinuclear fluorescence. Although all glitazones tested induce mitochondrial depolarization, the greatest effect was obtained with ciglitazone.

Downloaded from molpharm.aspetjournals.org at ASPET Journals on September 24, 2017

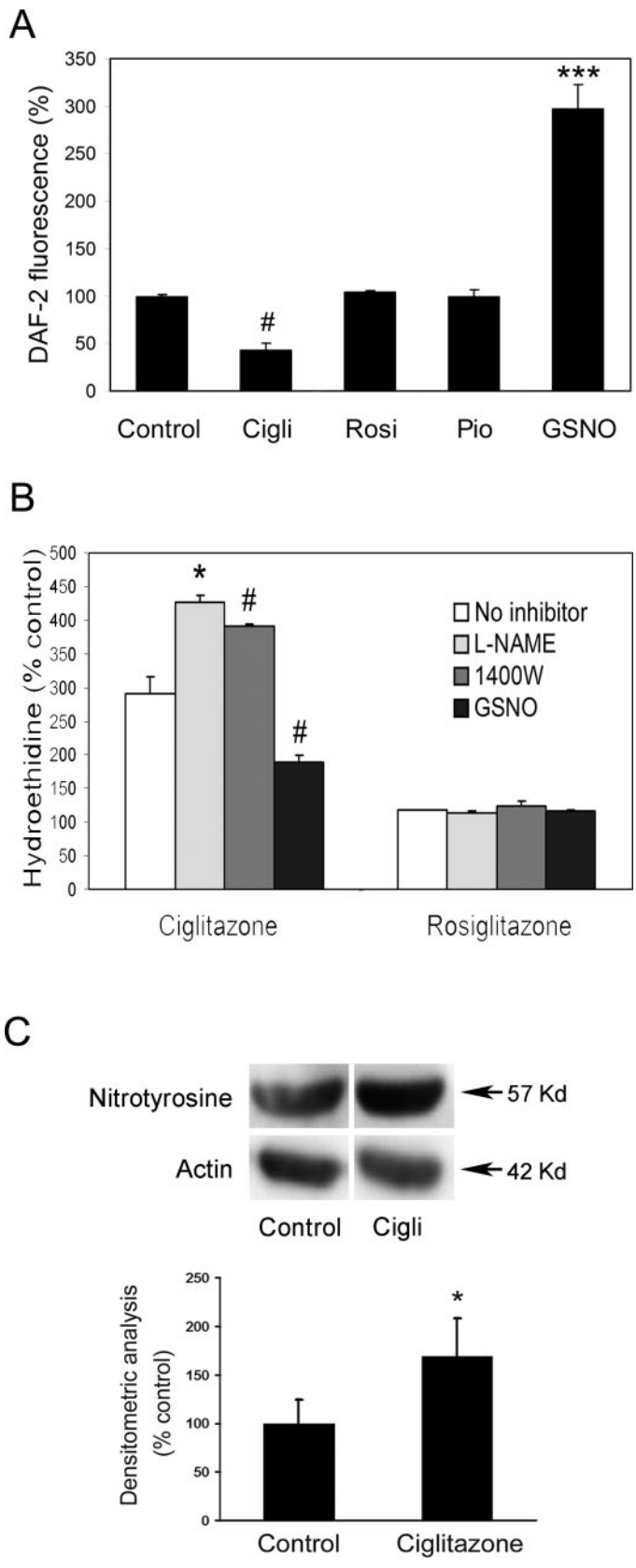

Fig. 6. Interaction between $O_2^{\cdot-}$ and NO in C6 cells treated with glitazones. A, C6 glioma cells were incubated with 10 μM ciglitazone, rosiglitazone, or pioglitazone during 15 min, whereas controls were treated with vehicle (0.02% Me_2SO) or the NO donor GSNO (500 μM). DAF-2 fluorescence, representing NO production, was evaluated by flow cytometry. B, flow cytometry analysis of HE fluorescence induced by a 15-min exposure to 10 μM ciglitazone or rosiglitazone. In addition, cells were preincubated for 2 h with an NOS inhibitor (500 μM L-NAME or 50 μM 1400W) or with 500 μM GSNO. C, C6 cells were treated for 3 h with 20 μM ciglitazone or vehicle, and proteins were extracted for nitrotyrosine detection by Western blotting. Densitometric analysis of nitrotyrosine immunoblots is also shown. In all panels, results are expressed as a percentage of controls treated with the appropriate vehicle. Data are presented as mean ± S.D., and statistically significant changes are indicated (#, $p < 0.05$; *, $p < 0.01$; ***, $p < 0.0001$).

mor necrosis factor-α in combination with lipopolysaccharide) in our experimental model. As shown in Supplemental Fig. S5B, both drugs are strong inhibitors of NO production in C6 cells. In addition, flow cytometry using the probe HE was used to evaluate $O_2^{\cdot-}$. Figure 6B shows that when NO synthesis was suppressed by preincubation with NAME or 1400W, HE oxidation in cells treated with 10 μM ciglitazone was enhanced reflecting an increase in $O_2^{\cdot-}$ levels. On the other hand, the oxidation of HE by $O_2^{\cdot-}$ was partially lost in the presence of the NO donor GSNO, probably because of the rapid interaction between both $O_2^{\cdot-}$ and NO, yielding $ONOO^-$. In contrast to ciglitazone, rosiglitazone was unable to modify HE fluorescence when administered either alone or in combination with NOS inhibitors or GSNO. Therefore, our results indicate that part of the $O_2^{\cdot-}$ generated by ciglitazone reacts with NO to form $ONOO^-$. A more direct way to demonstrate $ONOO^-$ formation was to quantify the presence of nitrotyrosine by Western blot in C6 cell protein extracts. Nitrosylated tyrosine residues were found to increase by ciglitazone treatment (Fig. 6C), supporting our contention of $ONOO^-$ generation. Furthermore, the band with enhanced nitration was found to comigrate with α-tubulin (Supplemental Fig. S6), in agreement with other reports (Eiserich et al., 1999; Zedda et al., 2004). The following mechanism could explain the accumulation of nitrotyrosine in tubulin over other proteins. Cells exposed to nitric oxide-derived species may have an increased pool of nitrotyrosine, which can be selectively incorporated into the extreme C terminus of α-tubulin by a post-translational mechanism in a reaction catalyzed by tubulin-tyrosine ligase (Eiserich et al., 1999; Zedda et al., 2004). Therefore, enhanced tubulin tyrosine nitrosylation in ciglitazone-treated C6 cells is probably caused by increased exposure to NO and funneling of the modified amino acid into this protein.

Although it is not a free radical, $ONOO^-$ is a potent oxidant that can potentially attack a wide range of biological molecules, causing lipid peroxidation, protein oxidation and nitration (as shown above), and induction of DNA strand breaks (Salgo et al., 1995). $ONOO^-$ also may impair the function of mitochondrial complex I (Riobó et al., 2001), which would be in accordance with the observed reduction in oxygen consumption with complex I substrates in the presence of ciglitazone. Therefore, to elucidate whether $O_2^{\cdot-}$ conversion to $ONOO^-$ by combination with NO affects cytotoxicity of glitazones in C6 glioma cells, the effect of NOS inhibition on cell viability was tested using propidium iodide (PI) staining of cells in a flow cytometry assay. The percentage of PI-positive cells increased as soon as 3 h after ciglitazone addition (Fig. 7). This effect was prevented by preincubation of cells with the NOS inhibitors L-NAME and 1400W, suggesting that $ONOO^-$ contributes to ciglitazone cytotoxicity. In conclusion, these results indicate that the fate of glioma cells treated with glitazones is affected by both $O_2^{\cdot-}$ and NO-derived reactive species.

Downloaded from molpharm.aspetjournals.org at ASPET Journals on September 24, 2017

Discussion

We use several strategies to identify the intracellular sources of ROS that are produced by glitazones in C6 glioma cells. The fluorescent probe H_2DCF is mainly sensitive to H_2O_2 and $ONOO^-$ (Hempel et al., 1999), whereas HE detects more specifically O_2^- (Rothe and Valet, 1990), particularly with a recent modification to the method (Robinson et al., 2006), thus providing complementary information on the nature of the oxygen species released. Ciglitazone enhanced fluorescence of both probes, whereas rosiglitazone and pioglitazone had only a significant effect on H_2DCF. Our interpretation is that ciglitazone increases HE fluorescence as a consequence of the higher levels of O_2^- produced, whereas rosiglitazone and pioglitazone would produce O_2^- at a slower rate. O_2^- may also be undetected if it is rapidly converted into H_2O_2 and/or $ONOO^-$. H_2DCF detects the latter species formed after treatment with ciglitazone, rosiglitazone, or pioglitazone. The fact that the glitazone-induced ROS increase was prevented by the uncoupler FCCP and by the nonmetabolizable 2-deoxy-glucose suggests that it is dependent on mitochondrial electron transport. As discussed below, glitazones may cause an inhibition of respiratory activity with substrates of complex I with two effects: one-electron transfer to O_2, with O_2^- formation, and a decrease in the $\Delta\Psi$m and mitochondrial pH. On the other hand, our studies with inhibitors of NADPH-oxidase and xanthine-oxidase rule out these extramitochondrial sources of ROS. Moreover, the mechanism is probably independent of PPARγ activation, as we (Pérez-Ortiz et al., 2004) and others (Brunmair et al., 2004) have suggested for several actions of glitazones.

All glitazones tested caused mitochondrial depolarization (ciglitazone being the most potent), measured by changes in TMRE fluorescence and subcellular distribution, and a simultaneous decrease in the mitochondrial pH, determined with the novel recombinant pH indicator mito-EYFP H148G. Such a rapid decrease in the mitochondrial membrane potential has also been reported after treatment of liver HepG2 cells with troglitazone (Bova et al., 2005), troglitazone or ciglitazone in mice liver mitochondria (Masubuchi et al., 2006), and ciglitazone in Jurkat, Raji, and human multiple myeloma cells (Kanunfre et al., 2004; Ray et al., 2004). Mitochondrial depolarization by glitazones could be a consequence of the opening of the mitochondrial permeability transition pore, because this mechanism has been proposed to explain the in vitro cytotoxicity of some glitazones (Masubuchi et al., 2006). However, the mitochondrial pore inhibitor cyclosporin A did not block the glitazone-induced depolarization in our case (results not shown). Because glitazones and FCCP cause mitochondrial depolarization, it is possible that they act as uncoupling agents similar to FCCP, which accelerates the electron transport by reducing the proton gradient. However, FCCP was unable to increase ROS levels in our experiments. In consequence, glitazones are likely to induce mitochondrial depolarization, a decrease in the mitochondrial pH gradient and ROS production in C6 cells by inhibiting electron transport rather than accelerating it. Other authors have proposed a direct interaction of glitazones with components of the electron transport chain, impairing the mitochondrial function. The highly lipophilic structure of glitazones would favor their accumulation in mitochondrial membranes (Brunmair et al., 2004).

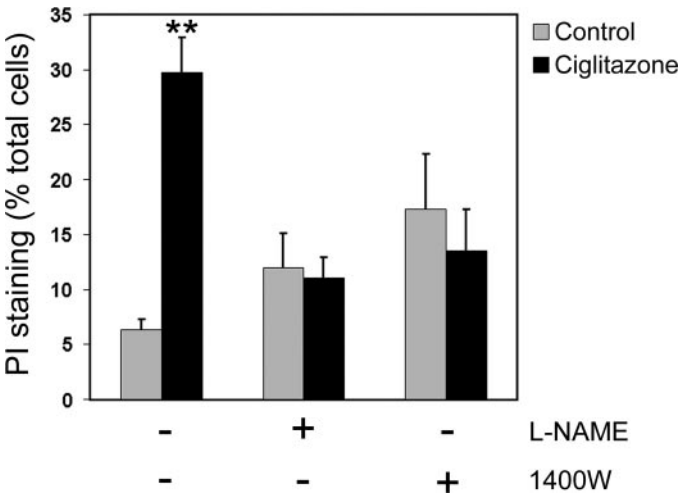

Fig. 7. Effect of NOS inhibitors on cell survival. C6 cells were stimulated for 3 h with 20 μM ciglitazone after a 2-h incubation with 500 μM L-NAME, 50 μM 1400W, or vehicle (Me_2SO). Viability was examined by flow cytometry after 10-min exposure to PI (10 μg/ml). Results represent a percentage of PI-positive cells and are expressed as mean ± S.D. Statistical significance of ciglitazone-treated cells versus respective controls is shown (**, $p < 0.001$).

Our results showing that ciglitazone, rosiglitazone, and pioglitazone reduce pyruvate and malate-dependent oxygen consumption in state 3 of respiration constitute a direct evidence of their inhibitory effect on mitochondrial function, involving respiratory complex I. Studies performed in muscle and liver homogenates and human cell lines support this contention and also point to complex I as the site inhibited by glitazones (Brunmair et al., 2004; Scatena et al., 2004). Therefore, ROS release, mitochondrial depolarization and pH decrease, and inhibition of oxygen consumption elicited by glitazones are probably caused by the inhibition of mitochondrial electron transport. A similar relationship has been proposed previously for rotenone (Li et al., 2003). We observed a correlation between the inhibition of mitochondrial oxygen consumption by individual glitazones and the magnitude of the ROS burst produced, with ciglitazone having the largest effect. O_2^- and other oxygen derivatives have been shown to block the function of several respiratory complexes (Riobó et al., 2001). Therefore, a positive feedback loop might be at play, in which ROS formed because of glitazone binding to mitochondria and inhibition of electron flow in complex I would enhance further ROS release.

ROS production by ciglitazone could not be blocked by any of the specific mitochondrial complex inhibitors used, including rotenone. A possible explanation is that ciglitazone inhibits electron transport upstream of the inhibition site of rotenone on complex I. Likely targets would be the flavin components of this complex, which are univalent electron carriers of sufficiently low redox potential to react with O_2 and produce O_2^- when they are reduced (Massey, 1994). ROS release by those components has been implicated in a rotenone model of Parkinson (Panov et al., 2005). On the other hand, the lack of effect of respiratory complex inhibitors on the induction of ROS by glitazones might be a consequence of the existence of multiple mitochondrial targets. A novel glitazone binding site in mitochondria has been demonstrated using tritiated pioglitazone and a photoaffinity cross-linker (Colca et al., 2004). The protein identified, termed "mitoNEET", is located in the mitochondrial fraction of rodent

Downloaded from molpharm.aspetjournals.org at ASPET Journals on September 24, 2017

brain, liver, and skeletal muscle. Part of the stimulatory effect of glitazones on ROS may also be caused by a feed-forward loop, in which ROS further interact with several mitochondrial loci. It is significant that O_2^- and other ROS show a well-defined affinity for the iron-sulfur clusters present at least in respiratory complexes I and II (Flint et al., 1993; Riobó et al., 2001). Moreover, $ONOO^-$ has the ability to inactivate several enzymes by stimulating tyrosine nitration and may cause damage to the electron transport chain (Riobó et al., 2001). We observed increased nitrotyrosine in glitazone-treated cells by Western blot.

We have shown that ciglitazone and rosiglitazone are lethal for human and rodent glioma cell lines but not for primary astrocytes in culture (Pérez-Ortiz et al., 2004). Pioglitazone has also shown selective inhibition of glioma growth in vivo (Grommes et al., 2006). Tumor cells are metabolically more active (Warburg effect) and subjected to a greater oxidative stress than nontumor astrocytes, which may explain their higher sensitivity to ROS-inducing stimuli such as glitazones. The mitochondrial mechanisms triggered by glitazones may inspire the development of new strategies for the treatment of tumors (Kondo et al., 2001). In fact, several antitumoral agents, such as anthracyclines, cisplatin, bleomycin, arsenic trioxide, and irradiation, show cytotoxicity based at least partly in the potentiation of ROS release (Pelicano et al., 2004).

Our previous work established that the enhancement of ROS production by glitazones is linked to cytotoxicity in C6 glioma cells (Pérez-Ortiz et al., 2004). In the present study, we detected O_2^- as the initial oxygen byproduct stimulated by glitazones. However, O_2^- is rapidly metabolized into H_2O_2 and/or $ONOO^-$, which are relatively stable oxidants with the capacity to pass cell membranes and induce cell damage. Because their cytotoxicity seems to be cell type-dependent, we devoted to determine which of these O_2^- derivatives were formed in C6 cells after glitazone treatment and their relative contribution to cytotoxicity. The interaction between NO and O_2^- to form $ONOO^-$ is favored over the O_2^- dismutation that results in H_2O_2 (Beckman and Koppenol, 1996). NO is the product of several cytoplasmic NOS, and a mitochondrial NOS isoform has also been reported (Riobó et al., 2002). C6 glioma cells have been shown to possess all cytosolic NOS isoforms (Barna et al., 1996; Yin et al., 2001; Ciampa et al., 2005), and we show the presence of iNOS by Western and functional analysis (cGMP levels).

Our results suggest that C6 glioma cells release NO that combines with O_2^- to form $ONOO^-$ and that reactive species derived from both O_2^- and NO are implicated in ciglitazone cytotoxicity. Upcoming therapeutic antitumoral strategies might derive from this and other work on glitazones. Furthermore, the present results lead us to subscribe to an appealing proposal (Brunmair et al., 2004) in which the decline in the mitochondrial function provoked by glitazones in several tissues may contribute to their antidiabetic effects, whose molecular mechanisms are still poorly characterized.

Acknowledgments

We gratefully acknowledge Ana M. Alonso for useful technical support, Dr. Laura Contreras for help with the oxygen consumption experiments, Dr. Joaquín Jordán for access to the oxygen electrode, and Dr. Jorgina Satrústegui for helpful discussion and careful reading of the manuscript.

References

Barna M, Komatsu T, and Reiss CS (1996) Activation of type III nitric oxide synthase in astrocytes following a neurotropic viral infection. *Virology* **223:**331–343.
Beckman JS and Koppenol WH (1996) Nitric oxide, superoxide, and peroxynitrite: the good, the bad, and ugly. *Am J Physiol* **271:**C1424–C1437.
Bova MP, Tam D, McMahon G, and Mattson MN (2005) Troglitazone induces a rapid drop of mitochondrial membrane potential in liver HepG2 cells. *Toxicol Lett* **155:**41–50.
Boveris A, Oshino N, and Chance B (1972) The cellular production of hydrogen peroxide. *Biochem J* **128:**617–630.
Brand MD, Affourtit C, Esteves TC, Green K, Lambert AJ, Miwa S, Pakay JL, and Parker N (2004) Mitochondrial superoxide: production, biological effects, and activation of uncoupling proteins. *Free Radic Biol Med* **37:**755–767.
Brunmair B, Staniek K, Gras F, Scharf N, Althaym A, Clara R, Roden M, Gnaiger E, Nohl H, Waldhausl W, et al. (2004) Thiazolidinediones, like metformin, inhibit respiratory complex I: a common mechanism contributing to their antidiabetic actions? *Diabetes* **53:**1052–1059.
Ciampa AR, de Prati AC, Amelio E, Cavalieri E, Persichini T, Colasanti M, Musci G, Marlinghaus E, Suzuki H, and Mariotto S (2005) Nitric oxide mediates anti-inflammatory action of extracorporeal shock waves. *FEBS Lett* **579:**6839–6845.
Colca JR, McDonald WG, Waldon DJ, Leone JW, Lull JM, Bannow CA, Lund ET, and Mathews WR (2004) Identification of a novel mitochondrial protein ("MitoNEET") cross-linked specifically by a thiazolidinedione photoprobe. *Am J Physiol Endocrinol Metab* **286:**E252–E260.
Delerive P, Fruchart JC, and Staels B (2001) Peroxisome proliferator-activated receptors in inflammation control. *J Endocrinol* **169:**453–459.
Eiserich JP, Estevez AG, Bamberg TV, Ye YZ, Chumley PH, Beckman JS, and Freeman BA (1999) Microtubule dysfunction by posttranslational nitrotyrosination of α-tubulin: a nitric oxide-dependent mechanism of cellular injury. *Proc Natl Acad Sci U S A* **96:**6365–6370.
Feinstein DL, Spagnolo A, Akar C, Weinberg G, Murphy P, Gavrilyuk V, and Dello RC (2005) Receptor-independent actions of PPAR thiazolidinedione agonists: is mitochondrial function the key? *Biochem Pharmacol* **70:**177–188.
Flint DH, Tuminello JF, and Emptage MH (1993) The inactivation of Fe-S cluster containing hydro-lyases by superoxide. *J Biol Chem* **268:**22369–22376.
Grommes C, Landreth GE, and Heneka MT (2004) Antineoplastic effects of peroxisome proliferator-activated receptor gamma agonists. *Lancet Oncol* **5:**419–429.
Grommes C, Landreth GE, Sastre M, Beck M, Feinstein DL, Jacobs AM, Schlegel U, and Heneka MT (2006) Inhibition of in vivo glioma growth and invasion by peroxisome proliferator-activated receptor γ agonist treatment. *Mol Pharmacol* **70:**1524–1533
Hempel SL, Buettner GR, O'Malley YQ, Wessels DA, and Flaherty DM (1999) Dihydrofluorescein diacetate is superior for detecting intracellular oxidants: comparison with 2′,7′-dichlorodihydrofluorescein diacetate, 5(and 6)-carboxy-2′,7′-dichlorodihydrofluorescein diacetate, and dihydrorhodamine 123. *Free Radic Biol Med* **27:**146–159.
Honda A, Adams SR, Sawyer CL, Lev-Ram V, Tsien RY, and Dostmann WR (2001) Spatiotemporal dynamics of guanosine 3′,5′-cyclic monophosphate revealed by a genetically encoded, fluorescent indicator. *Proc Natl Acad Sci U S A* **98:**2437–2442.
Kanunfre CC, da Silva Freitas JJ, Pompeia C, Goncalves d A, Cury-Boaventura MF, Verlengia R, and Curi R (2004) Ciglitazone and 15d PGJ2 induce apoptosis in Jurkat and Raji cells. *Int Immunopharmacol* **4:**1171–1185.
Kondo M, Oya-Ito T, Kumagai T, Osawa T, and Uchida K (2001) Cyclopentenone prostaglandins as potential inducers of intracellular oxidative stress. *J Biol Chem* **276:**12076–12083.
Li N, Ragheb K, Lawler G, Sturgis J, Rajwa B, Melendez JA, and Robinson JP (2003) Mitochondrial complex I inhibitor rotenone induces apoptosis through enhancing mitochondrial reactive oxygen species production. *J Biol Chem* **278:**8516–8525.
Massey V (1994) Activation of molecular oxygen by flavins and flavoproteins. *J Biol Chem* **269:**22459–22462.
Masubuchi Y, Kano S, and Horie T (2006) Mitochondrial permeability transition as a potential determinant of hepatotoxicity of antidiabetic thiazolidinediones. *Toxicology* **222:**233–239.
Nagano T (1999) Practical methods for detection of nitric oxide. *Luminescence* **14:**283–290.
Narayanan PK, Hart T, Elcock F, Zhang C, Hahn L, McFarland D, Schwartz L, Morgan DG, and Bugelski P (2003) Troglitazone-induced intracellular oxidative stress in rat hepatoma cells: a flow cytometric assessment. *Cytometry A* **52:**28–35.
Nishikawa T, Edelstein D, Du XL, Yamagishi S, Matsumura T, Kaneda Y, Yorek MA, Beebe D, Oates PJ, Hammes HP, et al. (2000) Normalizing mitochondrial superoxide production blocks three pathways of hyperglycaemic damage. *Nature* **404:**787–790.
Panov A, Dikalov S, Shalbuyeva N, Taylor G, Sherer T, and Greenamyre JT (2005) Rotenone model of Parkinson disease: multiple brain mitochondria dysfunctions after short term systemic rotenone intoxication. *J Biol Chem* **280:**42026–42035.
Pelicano H, Carney D, and Huang P (2004) ROS stress in cancer cells and therapeutic implications. *Drug Resist Updat* **7:**97–110.
Pérez-Ortiz JM, Tranque P, Vaquero CF, Domingo B, Molina F, Calvo S, Jordan J, Cena V, and Llopis J (2004) Glitazones differentially regulate primary astrocyte and glioma cell survival. Involvement of reactive oxygen species and peroxisome proliferator-activated receptor-γ. *J Biol Chem* **279:**8976–8985.
Radi R, Cassina A, and Hodara R (2002) Nitric oxide and peroxynitrite interactions with mitochondria. *Biol Chem* **383:**401–409.
Ray DM, Bernstein SH, and Phipps RP (2004) Human multiple myeloma cells

Downloaded from molpharm.aspetjournals.org at ASPET Journals on September 24, 2017

express peroxisome proliferator-activated receptor gamma and undergo apoptosis upon exposure to PPARgamma ligands. *Clin Immunol* **113:**203–213.
Riobó NA, Clementi E, Melani M, Boveris A, Cadenas E, Moncada S, and Poderoso JJ (2001) Nitric oxide inhibits mitochondrial NADH:ubiquinone reductase activity through peroxynitrite formation. *Biochem J* **359:**139–145.
Riobó NA, Melani M, Sanjuan N, Fiszman ML, Gravielle MC, Carreras MC, Cadenas E, and Poderoso JJ (2002) The modulation of mitochondrial nitric-oxide synthase activity in rat brain development. *J Biol Chem* **277:**42447–42455.
Robinson KM, Janes MS, Pehar M, Monette JS, Ross MF, Hagen TM, Murphy MP, and Beckman JS (2006) Selective fluorescent imaging of superoxide in vivo using ethidium-based probes. *Proc Natl Acad Sci U S A* **103:**15038–15043.
Rothe G and Valet G (1990) Flow cytometric analysis of respiratory burst activity in phagocytes with hydroethidine and 2′,7′-dichlorofluorescein. *J Leukoc Biol* **47:** 440–448.
Salgo MG, Bermudez E, Squadrito GL, and Pryor WA (1995) Peroxynitrite causes DNA damage and oxidation of thiols in rat thymocytes. *Arch Biochem Biophys* **322:**500–505.
Scatena R, Bottoni P, Martorana GE, Ferrari F, De SP, Rossi C, and Giardina B (2004) Mitochondrial respiratory chain dysfunction, a non-receptor-mediated effect of synthetic PPAR-ligands: biochemical and pharmacological implications. *Biochem Biophys Res Commun* **319:**967–973.
Schönfeld P and Reiser G (2006) Rotenone-like action of the branched-chain phytanic acid induces oxidative stress in mitochondria. *J Biol Chem* **281:**7136–7142.
Turrens JF (2003) Mitochondrial formation of reactive oxygen species. *J Physiol* **552:**335–344.
Votyakova TV and Reynolds IJ (2001) DeltaPsi$_m$-dependent and -independent production of reactive oxygen species by rat brain mitochondria. *J Neurochem* **79:** 266–277.
Yin JH, Yang DI, Chou H, Thompson EM, Xu J, and Hsu CY (2001) Inducible nitric oxide synthase neutralizes carbamylating potential of 1,3-bis(2-chloroethyl)-1-nitrosourea in C6 glioma cells. *J Pharmacol Exp Ther* **297:**308–315.
Yki-Järvinen H (2004) Thiazolidinediones. *N Engl J Med* **351:**1106–1118.
Zedda M, Lepore G, Gadau S, Manca P, and Farina V (2004) Morphological and functional changes induced by the amino acid analogue 3-nitrotyrosine in mouse neuroblastoma and rat glioma cell lines. *Neurosci Lett* **363:**190–193.

Address correspondence to: Dr. Juan Llopis, Facultad de Medicina, Universidad de Castilla-La Mancha, Avenida de Almansa 14, 02006 Albacete, Spain. E-mail: juan.llopis@uclm.es

Downloaded from molpharm.aspetjournals.org at ASPET Journals on September 24, 2017